Cytosolic Phosphorylation of Calnexin Controls Intracellular Ca^{2+} Oscillations via an Interaction with SERCA2b

H. Llewelyn Roderick,* James D. Lechleiter,‡ and Patricia Camacho*

*Department of Physiology, and ‡Department of Cellular and Structural Biology, University of Texas Health Science Center at San Antonio, San Antonio, Texas 78229-3900

Abstract. Calreticulin (CRT) and calnexin (CLNX) are lectin chaperones that participate in protein folding in the endoplasmic reticulum (ER). CRT is a soluble ER lumenal protein, whereas CLNX is a transmembrane protein with a cytosolic domain that contains two consensus motifs for protein kinase (PK) C/proline-directed kinase (PDK) phosphorylation. Using confocal Ca^{2+} imaging in *Xenopus* oocytes, we report here that coexpression of CLNX with sarco endoplasmic reticulum calcium ATPase (SERCA) 2b results in inhibition of intracellular Ca^{2+} oscillations, suggesting a functional inhibition of the pump. By site-directed mutagenesis, we demonstrate that this interaction is regulated by a COOH-terminal serine residue (S562) in CLNX. Furthermore, inositol 1,4,5-trisphosphate–mediated Ca^{2+} release results in a dephosphorylation of this residue. We also demonstrate by coimmunoprecipitation that CLNX physically interacts with the COOH terminus of SERCA2b and that after dephosphorylation treatment, this interaction is significantly reduced. Together, our results suggest that CRT is uniquely regulated by ER lumenal conditions, whereas CLNX is, in addition, regulated by the phosphorylation status of its cytosolic domain. The S562 residue in CLNX acts as a molecular switch that regulates the interaction of the chaperone with SERCA2b, thereby affecting Ca^{2+} signaling and controlling Ca^{2+}-sensitive chaperone functions in the ER.

Key words: phosphorylation • calnexin • ER lectin chaperones • Ca^{2+} ATPases • Ca^{2+} signaling

Introduction

Multiple cellular processes, including the control of gene transcription (Dolmetsch et al., 1998; Li et al., 1998), growth cone formation in neurons (Gomez and Spitzer, 1999), and activation of mitochondrial respiration (Robb-Gaspers et al., 1998) are encoded by spatial–temporal aspects of intracellular Ca^{2+} oscillations. Repetitive cytosolic Ca^{2+} transients in *Xenopus* oocytes are under the control of two major opposing factors: Ca^{2+} release through the inositol 1,4,5-trisphosphate receptor channel (IP_3R)[1] (Iino, 1990; Parker and Ivorra, 1990; Bezprozvanny et al., 1991; Finch et al., 1991) and Ca^{2+} reuptake into the ER Ca^{2+} store by the Ca^{2+} ATPases (Camacho and Lechleiter, 1993; MacLennan et al., 1997). Sarco endoplasmic reticulum calcium ATPase (SERCA)-type ATPases control the frequency of IP_3-induced Ca^{2+} oscillations in *Xenopus* oocytes (Camacho and Lechleiter, 1993). We have demonstrated previously that calreticulin (CRT), a lectin chaperone located in the ER, inhibits these oscillations and specifically targets SERCA2b (Camacho and Lechleiter, 1995a; John et al., 1998). The COOH terminus of SERCA2b, unlike that of SERCA2a, faces the ER lumen and contains an asparagine residue that forms part of a consensus site for N-linked glycosylation (N1036) (Gunteski-Hamblin et al., 1988) that we demonstrated is required for interaction with CRT (John et al., 1998). From these data we concluded that a functional interaction between CRT and SERCA2b may be required for inhibition of these oscillations.

CRT is a soluble lumenal ER protein, whereas calnexin (CLNX) and its testis-specific isoform, calmegin (CLMG), are type I transmembrane (TM) proteins (Michalak et al., 1992; Bergeron et al., 1994; Ohsako et al., 1994; Watanabe et al., 1994). This family of molecular chaperones is characterized by a lumenal domain that contains a motif of 17 amino acids repeated three times in CRT and four in CLNX and CLMG (Fliegel et al., 1989; Michalak et al., 1992; Ohsako et al., 1994; Watanabe et al., 1994). This do-

Address correspondence to Patricia Camacho, Department of Physiology, University of Texas Health Science Center at San Antonio, 7703 Floyd Curl Drive, San Antonio, TX 78229-3900. Tel.: (210) 567-6558. Fax: (210) 567-4410. E-mail: camacho@uthscsa.edu

[1]*Abbreviations used in this paper:* CLMG, calmegin; CLNX, calnexin; CRT, calreticulin; IP_3R, inositol 1,4,5-trisphosphate receptor; PDK, proline-directed kinase; PK, protein kinase; SERCA, sarco endoplasmic reticulum calcium ATPase; TM, transmembrane.

main is responsible for interaction of the chaperone with the monoglucosylated form of N-linked glycoproteins during protein folding in the ER (Vassilakos et al., 1998). The presence of this conserved domain led us to test whether CLNX, like CRT, also inhibits Ca^{2+} oscillations. Here, we demonstrate that CLNX inhibits Ca^{2+} oscillations in a manner consistent with inhibition of SERCA2b. Furthermore, as was the case for CRT, repetitive Ca^{2+} waves were unaffected by coexpression of CLNX with a SERCA2b mutant lacking the lumenal asparagine (SERCA2b-N1036A).

In contrast to CRT, CLNX has in its cytosolic domain consensus sites for phosphorylation by protein kinase (PK) C, casein kinase II, PKA, and proline-directed kinase (PDK) (Tjoelker et al., 1994; Wong et al., 1998). Recently, serine 562 located close to the COOH terminus of CLNX has been shown to support phosphorylation by the PDK, extracellular-signal regulated kinase 1 (ERK-1) (Wong et al., 1998), and was implicated in regulating an interaction of CLNX with ribosomal proteins (Chevet et al., 1999). The second residue, S485, faces the cytosol in proximity to the single TM segment. However, phosphorylation of this residue has eluded detection (Wong et al., 1998). Since activation of the IP_3 signaling pathway results in the production of both IP_3 and diacylglycerol (DAG), which is a known activator of PKC, we have also tested whether the two consensus motifs for PKC/PDK phosphorylation in CLNX play a role in the modulation of Ca^{2+} oscillations. Here we demonstrate that when the S562 is mutated to an unreactive alanine (S562A), Ca^{2+} oscillations are no longer inhibited, suggesting that S562 in CLNX plays a critical role in the regulation of Ca^{2+} oscillations. The presence of the S485 was required for regulation by S562. By immunoprecipitation of CLNX from ^{32}P-labeled oocytes, we demonstrate that CLNX becomes de-phosphorylated in S562 after mobilization of intracellular Ca^{2+} by IP_3. Furthermore, we demonstrate by coimmunoprecipitation that CLNX physically interacts with the COOH terminus of SERCA2b and that this interaction is reduced when asparagine 1036 is mutated to alanine. In addition, the interaction of CLNX with the COOH terminus of SERCA2b is significantly reduced by dephosphorylation treatment. Thus, we have identified a phosphorylated residue in CLNX that is dephosphorylated in a Ca^{2+}-sensitive manner, regulating SERCA2b to control ER store refilling and as a consequence, to maintain the integrity of the Ca^{2+}-sensitive protein folding machinery.

Materials and Methods

Construction of Expression Vectors

All cDNAs used in this study were subcloned between the 5′ and 3′ untranslated regions of *Xenopus laevis* β-globin into a vector (pHN) as described previously (Camacho and Lechleiter, 1995a,b). The cDNA encoding rat CLNX (Tjoelker et al., 1994) was excised from the pRc/CMV vector by BamHI and XbaI (restriction enzymes from GIBCO BRL) digestion and subcloned between the corresponding sites in a variant vector of pHN containing additional restriction sites in the multiple cloning site (pHNb-CLNX). Mutations in the consensus sites for PKC/PDK in CLNX were generated using the Quick-Change™ mutagenesis kit (Stratagene). The introduction of the desired mutation(s) in the plasmid recombinants was determined by automatic sequencing by the UTHSCA core facility. All oligonucleotides used to generate mutations were purchased from Operon Technologies. The CLNX-S485A mutant was generated using the forward primer with sequence 5′-CCTTGTGATCCTCTTCTGCTGTGCTGGAAAGAAACAGTCC-3′ and reverse primer with sequence 5′-GGACTGTTTCTTTCCAGCACAGCAGAAGAGGATCACAAGG-3′, and using as template pHNb-CLNX. The CLNX-S562A mutant was generated using the forward primer with sequence 5′-GGATGAAATTTTGAACAGAGCACCAAGAAACAGAAAGCCACGAAG- 3′, and the complementary reverse primer with sequence 5′-CTTCGTGGCTTTCTGTTTCTTGGTGCTCTGTTCAAAATTTCATCC-3′ and pHNb-CLNX was again used as template. The double mutant CLNX-S485A/S562A was generated by exchanging the RsaI to NheI fragment containing the CLNXS562A mutation for the equivalent wild-type cDNA in the vector pHNb-CLNXS485A backbone. The presence of both mutations was confirmed by sequencing. The CLNX cytosolic peptide was generated by conventional PCR amplification of an internal fragment spanning the S562 PKC consensus site (A537 to the COOH terminus). This primer had sequence 5′-ACTGGGATCCATGGATGCTGAAGAAGATGGTGG-3′ and incorporated a BamHI site at its 5′ end. The antisense oligonucleotide had sequence 5′-GCTTAGAGACTCCATTC-3′, which is complementary to the 3′ untranslated region of *Xenopus* β-globin. The product of this PCR amplification was digested with BamHI and XbaI and after purification was subcloned into vector pHNb and similarly digested (plasmid pHNb-$CLNX_{cyt}$). The expression vector for SERCA2b has been described elsewhere (Camacho and Lechleiter, 1995a; John et al., 1998). The COOH-terminal domain mutants of SERCA2b and SERCA2b-N1036A spanning TM segments 9–11 were generated by PCR using as forward primer 5′-ACTGGGATCCATGCCCCCCTGGGAGAACATCTGGCTCG-3′ incorporating a BamHI site and as the reverse primer 5′-GCTTAGAGACTCCATTC-3′, which is complementary to the 3′ untranslated region of *Xenopus* β-globin present in the template (pHN-SERCA2b). The PCR products were digested with BamHI and HindIII and ligated to the similarly digested *Xenopus* expression vector, pHN. The final constructs encode the COOH terminus of SERCA2b and SERCA2b-N1036A starting at the methionine residue 924, which is located just before TM9 (Bayle et al., 1995). The plasmids were named pHN-SERCA2b/TM9-11 and pHN-SERCA2b-N1036A/TM9-11. A similar strategy was followed to generate the SERCA 2a/TM9-10 using as PCR template plasmid pHN-SERCA2a (John et al., 1998). All vectors generated were fully sequenced automatically by the core facility at the UTHSCSA.

In Vitro Transcriptions and Oocyte Protocols

Synthetic mRNA was prepared as described previously (Camacho and Lechleiter, 1995a). Plasmids were linearized with NotI, except for plasmid pHNb-CLNX, which was linearized by NheI digestion. Transcription initiated at the T7 promoter was performed using the Megascript™ high yield transcription kit and capped with m7G(5′)ppp(5′′) (both from Ambion). All synthetic mRNAs were resuspended at a concentration of 1.5–2.0 μg/μl and stored in aliquots of 3 μl at −80°C. Stage VI defolliculated oocytes were injected with a bolus of 50 nl of mRNA using a standard positive pressure injector (Nanoject; Drummond Scientific). After mRNA injection, oocytes were cultured for 5–7 d until Ca^{2+} imaging was performed. The culture media contained 50% L-15 Media (GIBCO BRL) supplemented with antibiotics and was changed daily.

Western Blot Analysis

Oocyte extracts used in Western blots were prepared from pools of 10 oocytes as described previously (Camacho and Lechleiter, 1995a). To determine equal loading, membranes were stained with Ponceau S and a single band was densitometrically analyzed for use as an internal standard for equal loading in subsequent gels. To detect CLNX the membranes were probed with the rabbit anti-CLNX antibody (SPA-860; StressGen Biotechnologies). To detect the SERCA2b antigen, we used a polyclonal rabbit anti-SERCA antibody (N1; gift of J. Lytton, University of Calgary Health Science Center, Calgary, Alberta, Canada). HRP-conjugated secondary antibodies were used in all Western blots (Jackson ImmunoResearch Laboratories, Inc.) and visualized by enhanced chemiluminescence (Pierce Chemical Co.).

Immunoprecipitations of γ-^{32}P–labeled CLNX

Groups of oocytes (n = 30, each) overexpressing the same constructs used in Ca^{2+} imaging experiments were injected with a 50-nl bolus of [γ-^{32}P]ATP (1:2 dilution of a 150-mCi/mL stock; 6,000 Ci/mM; New England Biolabs, Inc.). After a 10-min period of equilibration, half of the oocytes

in each group were injected with IP_3 (~300 nM final; Calbiochem). Oocytes were instantly frozen on dry ice 6 min after the IP_3 injection. During these treatments, oocytes were maintained in ND96 buffer which contained 1 mM EGTA, 96 mM NaCl, 2 mM KCl, 2 mM $MgCl_2$, 5 mM Hepes, pH 7.5. Membrane extracts were prepared as follows: oocytes were homogenized in lysis buffer (40 mM Tris-HCl, pH 7.5, 50 mM NaCl, 10 mM $MgCl_2$, 2 mM EDTA, 0.5 mM EGTA) supplemented with phosphatase inhibitors (10 mM NaF, 0.4 mM Na_3VO_4, 0.1 mM $ZnCl_2$, 1 mM $NaPP_i$) and the protease inhibitors (2 mM PMSF, 20 μM leupeptin, and 150 μM pepstatin A final). The oocytes were extracted twice in volumes of 300 μl, with the particulate fraction being removed by centrifugation at 10,000 *g* for 15 s between each extraction. The membrane fraction was isolated by centrifugation for 1 h at 100,000 *g*. Membrane proteins were extracted at room temperature in solubilization buffer (10 μl per oocyte) consisting of lysis buffer containing 1% IGEPAL (Sigma Chemical Co.) and 1% SDS for 20 min. The soluble fraction was then isolated by centrifugation at 10,000 *g* for 5 min. After a fivefold dilution in lysis buffer, 10 μl of a 50% suspension of protein A–Sepharose (pretreated by incubation 3 × 20 min in 5% BSA) was added to the membrane fraction. After over-end rotation at room temperature for 2 h, the protein A–Sepharose was removed by centrifugation. The CLNX antibody was added at a dilution of 1:250 and incubated with over-end rotation at 4°C overnight. To the cell lysate, 8 μl of the 50% suspension of pretreated protein A–Sepharose was added and incubated with over-end rotation for 1 h at room temperature. The immune complexes were washed three times with lysis buffer containing 1% IGEPAL and harvested by centrifugation and eluted from the protein A–Sepharose by boiling for 4 min in Laemmli SDS sample buffer. The proteins were separated by SDS-PAGE through an 8% gel. After the gel was fixed and dried, the proteins were visualized by autoradiography.

In Vitro Translations and Glycosylation Analysis

Messenger RNA was diluted to 0.1 μg/μl and translated for 45 min in a rabbit reticulocyte lysate translation system supplemented with canine pancreatic microsomes and L-[^{35}S]methionine according to the instructions of the manufacturer (Promega). To prevent further initiation of translation, m7G(5′)ppp(5′′) (Ambion) was added to a final concentration of 2 mM and incubated for 5 min at 30°C. Nascent chains were released from ribosomes by treatment with puromycin (Fisher Scientific), which was added to a concentration of 1 mM and incubated for 5 min at 30°C. To inhibit ongoing translation, emetine (Sigma Chemical Co.) was added to a final concentration of 2 mM and incubated on ice for 5 min. Finally, the microsomal fraction was isolated by ultracentrifugation at 125,000 *g* for 12 min through a high salt–sucrose cushion using a Beckman Optima TLX ultracentrifuge in a TLA 45 rotor (Oliver et al., 1996).

To determine whether the COOH terminus of SERCA2b was glycosylated, microsomes were isolated from in vitro translation reactions programmed with appropriate mRNAs as described above. The isolated microsomes were solubilized by boiling in endo H denaturing buffer (New England Biolabs, Inc.) for 10 min. To half of each reaction, one tenth volume of 10× G5 buffer and 1 μl of endo H_f was added and incubated at 37°C for 2 h. The samples were then subjected to SDS-PAGE and fluorography.

Coimmunoprecipitations and Dephosphorylations

Microsomes from the mRNA-programmed translations were solubilized in immunoprecipitation lysis buffer containing 1% Triton X-100, 10 mM Tris-HCl, pH 7.6, 140 mM NaCl, 0.2 mM [4-(zaminoethyl)benzene sulfonylfluoride, HCl] (AEBSF; Calbiochem) for 45 min at 4°C. After centrifugation at 16,000 *g*, the supernatant was retained, diluted fivefold in immunoprecipitation buffer without Triton X-100 and precleared by incubation with 10 μl of a 50% suspension of protein A/G PLUS agarose (Santa Cruz Biotechnology, Inc.) with over-end rotation at 4°C for 1 h. The agarose was discarded after centrifugation at 1000 *g* for 5 min. To the supernatant, 3 μl of anti-CLNX antibody (C3; gift of J. Bergeron, McGill University, Montreal, Canada) was added and incubated with over-end rotation at 4°C overnight. Protein A/G PLUS agarose (20 μl of a 50% suspension) was added and incubated with over-end rotation at 4°C for 1 h. The immune complexes were harvested by centrifugation at 1,000 *g* for 5 min and washed twice with immunoprecipitation buffer containing 0.1% Triton X-100 and once without Triton X-100. The immune complexes were resuspended in sample buffer containing 38 mM DTT to denature the proteins, boiled for 5 min and subjected to 15% SDS-PAGE. The gels were fixed, incubated in Amplify™ (Amersham Pharmacia Biotech), dried, and visualized by fluorography.

For dephosphorylation reactions, microsomes from the SERCA2b/TM9-11 or the SERCA2b-N1036A/TM9-11 translations were resuspended in 50 μl of immunoprecipitation buffer containing 2 mM $MgCl_2$ without Triton X-100. 5 U (1 U/μl) of calf intestinal alkaline phosphatase (Boehringer) was added and dephosphorylation was allowed to proceed at 30°C for 20 min. The microsomes were isolated by centrifugation through a high salt/sucrose cushion and processed for coimmunoprecipitation and SDS-PAGE as described above. All coimmunoprecipitations and dephosphorylation experiments were performed on at least three independent occasions, and the standard error bars are indicated for densitometric measurements on the corresponding figures.

Confocal Imaging of Intracellular Ca^{2+}

Ca^{2+} wave activity was imaged with the fluorescent Ca^{2+} indicator, Oregon green I (12.5 μM final concentration assuming an oocyte volume of 1 μl) (Molecular Probes, Inc.). With exception to experiments using pyruvate malate–treated oocytes, confocal imaging was performed using a NORAN OZ confocal laser scanning microscope at zoom 0.7 attached to a Nikon 200 Eclipse inverted microscope. A 20× (0.75 NA) water immersion Nikon objective was used and images were collected at 0.5-s intervals. The confocal slit was set at 50 μm. Confocal imaging of pyruvate malate–treated oocytes was performed using a Zeiss confocal laser scanning microscope (LSM310) at zoom 2 attached to a Zeiss upright Axioplan microscope. A 10× objective was used and images were collected at 0.5-s intervals. Images were analyzed with ANALYZE software (Mayo Foundation) on a Silicon Graphics O2 workstation. Ca^{2+} increases were initiated by injection of a 50-nl bolus of 6 μM IP_3 (~300 nM final) (Calbiochem). All images were acquired in ND96 containing 1 mM EGTA (Sigma Chemical Co.) without extracellular Ca^{2+}.

Statistical Analysis

Statistical significance was determined by using the *t* test and the Chi-square test where appropriate. Significance level was accepted at $P < 0.05$.

Results

Overexpression of CLNX in Xenopus Oocytes Inhibits Intracellular Ca^{2+} Oscillations

Although CRT has been shown to modulate different aspects of Ca^{2+} signaling (Bastianutto et al., 1995; Mery et al., 1996; Coppolino et al., 1997; Fasolato et al., 1998; John et al., 1998; Roderick et al., 1998; Mesaeli et al., 1999), most of these effects were attributed to CRT's ability to bind Ca^{2+} with high capacity (Baksh and Michalak, 1991; Bastianutto et al., 1995; Mery et al., 1996; Coppolino et al., 1997; Fasolato et al., 1998; Roderick et al., 1998; Mesaeli et al., 1999). However, we demonstrated by deletion mutagenesis that the inhibition of Ca^{2+} waves observed when CRT is overexpressed in *Xenopus* oocytes survives deletion of the high capacity Ca^{2+} binding C-domain (Camacho and Lechleiter, 1995a; John et al., 1998). Since CLNX shares homology to CRT on the P-domain and both have been characterized as lectin chaperones, we tested whether CLNX would also modulate Ca^{2+} oscillations. CLNX-overexpressing oocytes injected with IP_3 (300 nM final) were imaged confocally 5 d after mRNA injection. Very few of these oocytes exhibited Ca^{2+} oscillations (12%; $n = 17$). These oscillations are rarely observed in control, nonoverexpressing oocytes after 6 d of culture (17%; $n = 18$). Thus, we tested the effects of CLNX overexpression under conditions that reliably elicit robust Ca^{2+} oscillations (i.e., overexpression of SERCA pumps or energization of mitochondria with pyruvate/malate) (Camacho and Lechleiter, 1993, 1995a; John et al., 1998;

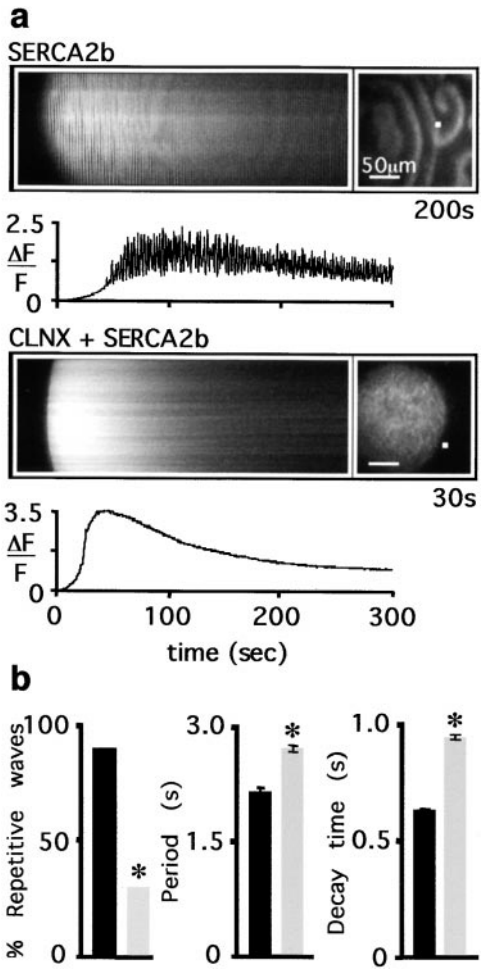

Figure 1. Overexpression of CLNX in *Xenopus* oocytes inhibits repetitive Ca^{2+} waves. (a) Confocal Ca^{2+} imaging in a control oocyte overexpressing rat SERCA2b shows high frequency Ca^{2+} oscillations after an injection of IP_3 (~300 nM final). Inhibition of Ca^{2+} oscillations is also shown for a representative oocyte coexpressing CLNX + SERCA2b. In this and subsequent figures, the top image contains a spatio–temporal stack of Ca^{2+} wave activity followed to the right by a representative confocal image of Ca^{2+} wave activity at the indicated timepoint. Bar, 50 μm. Also in this and subsequent figures, the trace under each image represents the change in fluorescence from resting levels (ΔF/F) shown as a function of time. The white square represents the 5 × 5 pixel area used in determining ΔF/F. (b) The percentage of oocytes exhibiting repetitive Ca^{2+} wave activity was decreased in oocytes coexpressing CLNX + SERCA2b (n = 63, 30%), relative to oocytes overexpressing SERCA 2b alone (n = 52, 88%) (left). The asterisk indicates statistical significance in comparison to oocytes overexpressing SERCA2b alone, $P < 0.005$ (Chi-square test). In this figure and subsequent histograms, the color convention used is as follows: black for SERCA 2b and light gray for CLNX + SERCA2b overexpressing oocytes. Detailed analysis of Ca^{2+} waves was performed only on those oocytes that exhibited repetitive Ca^{2+} waves. Compared with oocytes overexpressing SERCA 2b alone, overexpression of CLNX + SERCA2b increased the period between waves (middle) and the decay time of individual waves (right). The asterisk denotes a statistical significant difference $P < 0.05$ (t test) in comparison to control oocytes overexpressing SERCA2b alone (see also Table I).

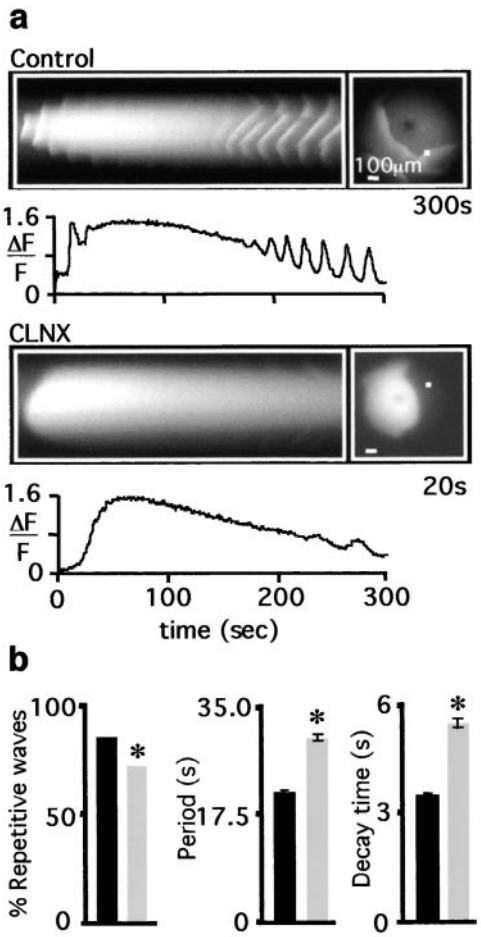

Figure 2. Overexpression of CLNX in *Xenopus* oocytes inhibits repetitive Ca^{2+} waves induced by mitochondrial energization. (a) Confocal Ca^{2+} imaging of a control oocyte (IP_3 ~300 nM final) energized previously with pyruvate malate (10 mM final). In this representative oocyte, a Ca^{2+} tide is followed by low-frequency Ca^{2+} oscillations. Ca^{2+} oscillations are inhibited in a representative oocyte overexpressing CLNX. Bar, 100 μm. (b) The percentage of oocytes exhibiting repetitive Ca^{2+} wave activity was decreased in oocytes overexpressing CLNX (n = 18, 71%), relative to control oocytes (n = 25, 84%) (left). The asterisk indicates statistical significance in comparison to oocytes overexpressing SERCA2b alone, $P < 0.05$ (Chi-square test). Detailed analysis of Ca^{2+} waves was performed only on those oocytes that exhibited repetitive Ca^{2+} activity. Compared with control oocytes, overexpression of CLNX increased the period between waves (middle) and the decay time of individual waves (right). The asterisk denotes a statistical significant difference $P < 0.05$ (t test) in comparison to control oocytes (see also Table II).

Jouaville et al., 1995). Compared with oocytes overexpressing SERCA2b alone, oocytes coexpressing CLNX + SERCA2b displayed inhibition of high frequency Ca^{2+} oscillations (Fig. 1 a). A large percentage of oocytes overexpressing SERCA2b alone exhibited high-frequency repetitive Ca^{2+} waves (88%; n = 52), whereas this percentage was significantly lower in CLNX + SERCA2b oocytes (30%; n = 63) (Fig. 1 b, left, and Table I). In addition, in comparison to SERCA2b-overexpressing oocytes, CLNX + SERCA2b coexpressing oocytes appear to have a more rapid initial rise in cytosolic Ca^{2+}, suggesting that in these

Table I. Detailed Analysis of Ca^{2+} Wave Activity in Oocytes that Exhibited Repetitive Ca^{2+} Waves

	Oocytes per group	Oocytes displaying oscillations	Wave Period	Decay Time
	n	%	*s*	*s*
SERCA2b	52	88.0	2.49 ± 0.01	0.62 ± 0.01
CLNX + SERCA2b	63	30.0*	3.13 ± 0.02*	0.93 ± 0.01*
CLNX-S562A + SERCA2b	36	92.0‡	3.06 ± 0.02	0.73 ± 0.01‡
CLNX-S485A + SERCA2b	27	15.0	3.45 ± 0.04	1.05 ± 0.02
CLNX-S562A/S485A + SERCA2b	34	26.5	3.42 ± 0.02	1.07 ± 0.01§
$CLNX_{cyt}$ + CLNX + SERCA2b	18	72.0‖	2.97 ± 0.03	0.79 ± 0.01‖
SERCA2b-N1036A	20	100	1.88 ± 0.01¶	0.35 ± 0.002
CLNX + SERCA2b-N1036A	19	100	2.10 ± 0.03	0.46 ± 0.007**

Mean ± SEM. *n*, total number of oocytes per category. Percentage is the percent of *n*. The statistical significance was analyzed with a Chi-square test for comparisons related to the percentage of oocytes displaying oscillations ($P < 0.005$). All other comparisons were tested for statistical significance using *t* test, and *P* values are indicated.
*CLNX + SERCA2b is not equivalent to SERCA2b ($P < 0.005$).
‡CLNX-S562A + SERCA2b is not equivalent to CLNX + SERCA2b ($P < 0.01$).
§CLNX-S562A/S485A + SERCA2b is not equivalent to CLNX + SERCA2b ($P < 0.05$).
‖$CLNX_{cyt}$ + CLNX + SERCA2b is not equivalent to CLNX + SERCA2b ($P < 0.05$).
¶SERCA2b-N1036A is not equivalent to SERCA2b ($P < 0.05$).
**SERCA2b-N1036A is not equivalent to CLNX + SERCA2b-N1036A ($P < 0.05$).

oocytes, rapid amplification of Ca^{2+} release occurs because the Ca^{2+} ATPase is inhibited. Therefore, we performed measurements of interwave period and decay time of individual waves ($t_{1/2}$), which reflect the Ca^{2+} uptake process (John et al., 1998). Compared with control oocytes overexpressing SERCA2b alone, oocytes coexpressing CLNX + SERCA2b had statistically significant longer interwave periods and longer decay times for individual waves (Fig. 1 b, middle and right, and Table I).

Energization of mitochondria by injection of pyruvate malate (10 mM final) results in a Ca^{2+} tide followed by robust, low-frequency Ca^{2+} waves (Fig. 2 a). Overexpression of CLNX alone in oocytes injected with pyruvate malate results in inhibition of Ca^{2+} oscillations. Specifically, the percentage of oocytes displaying oscillations was significantly reduced by CLNX overexpression in relation to control nonoverexpressing oocytes (Fig. 2 b, left, and Table II). More importantly, interwave periods and decay times for individual waves were significantly increased in CLNX-overexpressing oocytes (Fig. 2 b, middle and right, and Table II).

The functional interaction of CRT with SERCA2b requires the presence of a luminal asparagine in the pump (John et al., 1998). To determine whether the mechanism of inhibition by CLNX also involves this asparagine, we overexpressed SERCA2b-N1036A and compared these oocytes to oocytes coexpressing CLNX + SERCA2b-N1036A (Fig. 3). High-frequency repetitive Ca^{2+} waves without a preceding tide were observed in all of these oocytes (Table I). As was the case with CRT (John et al., 1998), CLNX did not inhibit Ca^{2+} oscillations when coexpressed with SERCA2b-N1036A. Thus, the percentage of oocytes exhibiting repetitive Ca^{2+} wave activity was unchanged in oocytes coexpressing CLNX ($n = 19$; 100%), relative to control oocytes ($n = 20$; 100%) (Table I). In addition, there is no statistical difference between SERCA2b-N1036A and CLNX + SERCA2b-N1036A overexpressing oocytes in interwave periods (Table I). Thus, both members of this family of chaperones appear to functionally interact with SERCA2b, and mutagenesis of the lumenal asparagine interferes with the manifestation of this inhibitory effect.

Table II. Analysis of Ca^{2+} Wave Activity in Pyruvate Malate–treated Oocytes that Exhibited Repetitive Ca^{2+} Waves

	Oocytes per group	Oocytes displaying oscillations	Wave Period	Decay Time
	n	%	*s*	*s*
Control	25	84	20.55 ± 0.45	3.41 ± 0.06
CLNX	18	71*	29.49 ± 0.57*	5.39 ± 0.09*

Mean ± SEM. *n*, total number of oocytes per category. Percent is the percent of *n*. The statistical significance was analyzed with a Chi-square test for comparisons related to the percentage of oocytes displaying oscillations ($P < 0.005$). All other comparisons were tested for statistical significance using *t* test, and *P* values are indicated.
*CLNX is not equivalent to control ($P < 0.05$).

CLNX Physically Interacts with the COOH Terminus of SERCA2b

In the preceding experiments we demonstrated a functional interaction between CLNX and SERCA2b but not with SERCA2b-N1036. In the modulation of protein folding, CLNX has been shown to interact with substrates by two mechanisms, either by a lectin interaction with the monoglucosylated N-linked glycans, or by a more classical chaperone protein–protein interaction (Helenius et al., 1997; Ihara et al., 1999). Thus, our results with the N1036A mutant could be attributed either to the removal of the N-linked glycan or to a change in charge, which undermines the interaction of the Ca^{2+} ATPase with CLNX. To characterize this interaction, we first determined whether SERCA2b is glycosylated. We generated constructs encoding the COOH terminus of SERCA2b and its N1036A mutant starting at TM9 (i.e., SERCA2b/TM9-11 and SERCA2b-N1036A/TM9-11), as well as of SERCA2a/TM9-10 to use as control (Gunteski-Hamblin et al., 1988). Correct polytopic insertion of the translation products in the ER membrane has been demonstrated previously for similar constructs in microsomes (Bayle et al., 1995). After mRNA synthesis, translation was performed in rabbit reticulocyte lysate in the presence of canine pancreatic microsomes. All constructs were efficiently translated and run at the correct predicted molecular masses (SERCA2b and SERCA2b-N1036A/TM9-11, ~13.2 kD; and SERCA2a ~7.2 kD). Posttranslational processing was observed on a

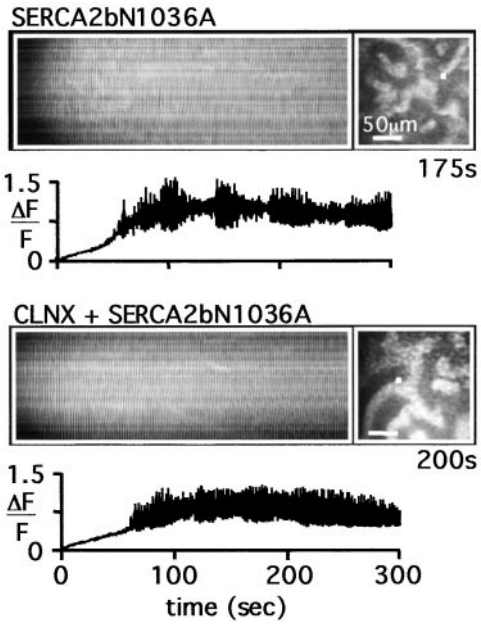

Figure 3. CLNX does not inhibit Ca^{2+} oscillations induced by overexpression of the SERCA2b-N1036A mutant. Confocal Ca^{2+} imaging in an oocyte overexpressing SERCA2b-N1036A after an injection of IP_3 (~300 nM final) shows high-frequency Ca^{2+} oscillations (top). These oscillations are not inhibited in oocytes coexpressing CLNX + SERCA2b-N1036A (bottom). Bar, 50 μm.

protein glycosylated on three asparagine residues that served as positive control (glycosylated *S. cerevisiae* α factor, ~30 kD). SERCA2b and the N1036A mutant migrate at a similar rate, indicating that SERCA2b might not be glycosylated (Fig. 4 a). To corroborate this, we treated in vitro translated SERCA2b/TM9-11 and SERCA2b-N1036A/TM9-11 products with endoglycosidase H (endo H). Under the experimental conditions, *S. cerevisiae* α factor underwent de-glycosylation by endo H (Fig. 4 b). However, endo H treatment did not alter the mobility of SERCA2b/TM9-11 or of SERCA2b-N1036A/TM9-11, indicating that SERCA2b is not glycosylated.

Since CLNX has been shown to interact also via protein–protein interactions regardless of whether the substrate is glycosylated (Ihara et al., 1999), the possibility remained that CLNX would interact with the COOH terminus of SERCA2b. To test this hypothesis, we performed coimmunoprecipitations in which endogenous CLNX present in the pancreatic microsomes was immunoprecipitated with a CLNX-specific antibody. Coimmunoprecipitated proteins were subsequently detected by fluorography. SERCA2b, and to a significantly lower extent, SERCA-N1036A were coimmunoprecipitated (0.61 ± 0.02, $P < 0.005$, $n = 5$) (Fig. 4 c). More importantly, no interaction with the COOH terminus of SERCA2a was de-

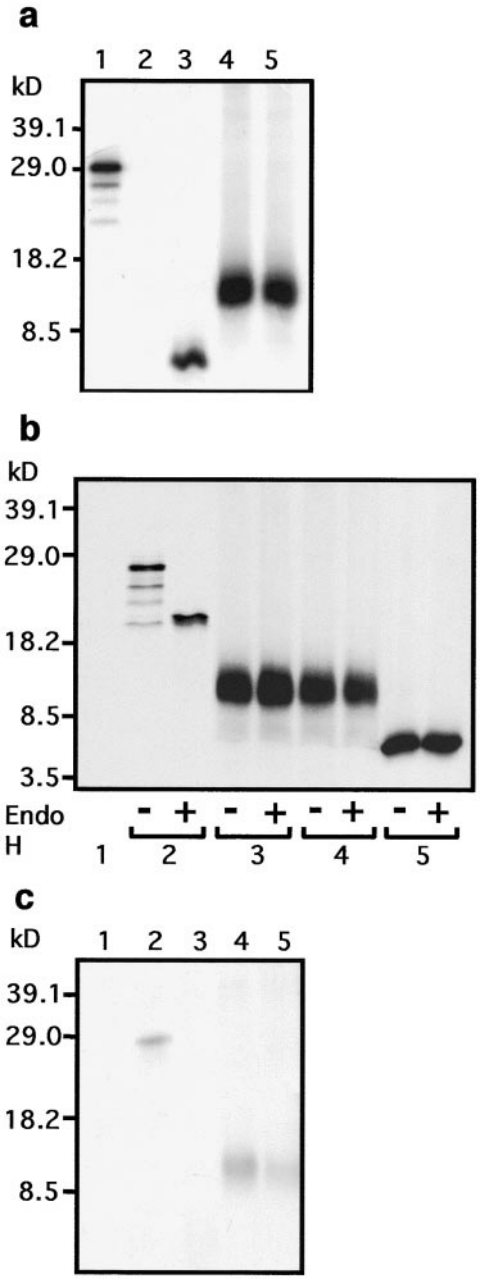

Figure 4. CLNX coimmunoprecipitates with the COOH terminus of SERCA2b. In vitro translations of synthetic mRNAs were performed in rabbit reticulocyte lysate supplemented with canine pancreatic microsomes and L-[^{35}S]methionine. Samples were subjected to 15% SDS-PAGE and detected by fluorography. (a) Membrane fractions isolated from in vitro translation reactions were loaded as follows: *S. cerevisiae* α factor (lane 1), negative control without RNA (lane 2), SERCA2a/TM9-10 (lane 3), SERCA2b/TM9-11 (lane 4), and SERCA2b-N1036A/TM9-11 (lane 5). (b) Endo H treatment demonstrates that the COOH terminus of SERCA2b is not glycosylated. Samples were loaded as follows: negative control without mRNA (lane 1), paired samples were loaded ± endo H as follows: *S. cerevisiae* α factor (second set of lanes), SERCA2b/TM9-11 (third set of lanes), SERCA2b-N1036A/TM9-11 (fourth set of lanes), and SERCA2a/TM9-10 (fifth set of lanes). (c) Coimmunoprecipitations of CLNX with SERCA COOH terminus constructs demonstrates an interaction of CLNX with SERCA2b, a reduced interaction with the SERCA2b-N1036A mutant, but no interaction with SERCA2a. Lanes were loaded as follows: negative control without RNA in the translation (lane 1), *S. cerevisiae* α factor (lane 2), SERCA2a/TM11-10 (lane 3), SERCA2b/TM9-11 (lane 4), and SERCA2b-N1036A/TM9-11 (lane 5).

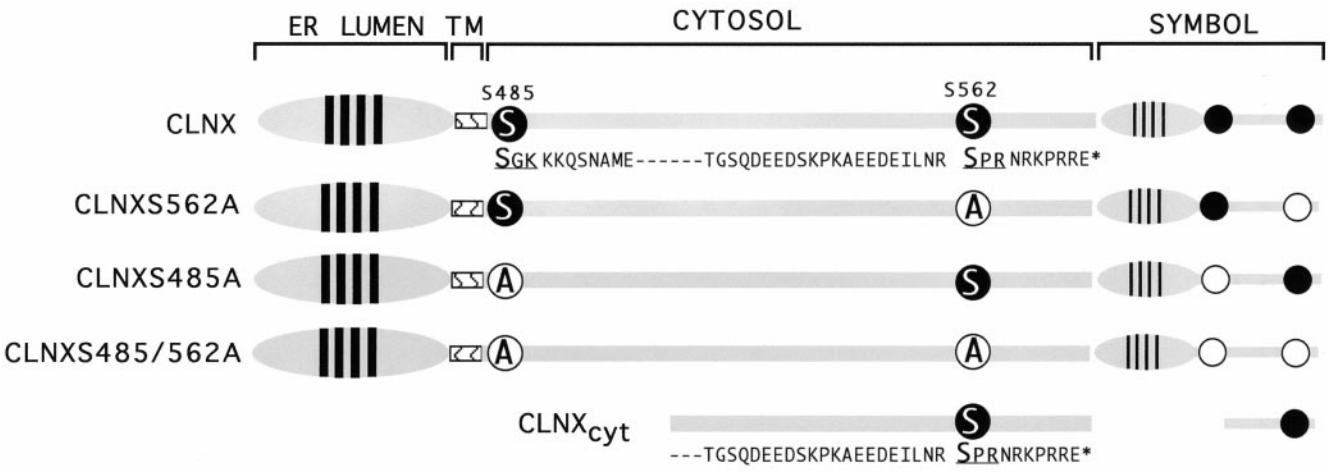

Figure 5. Mutagenesis of consensus sites for phosphorylation by PKC/PDK in CLNX. The ER lumenal, single TM, and cytosolic domain boundaries for CLNX are indicated. Partial sequence of the cytosolic domain is shown in single letter amino acid code. PKC phosphorylation consensus sites are indicated in bold and underline. Specific phosphorylated residues are shown in larger font and depicted as filled circles. Sequence mutations generated are indicated in amino acid code and depicted by clear circles. The full sequence and position relative to wild-type CLNX is shown for the $CLNX_{cyt}$ cytosolic peptide. To the right of each construct, the corresponding symbol is given and is used in subsequent figures.

tected. Finally, the *S. cerevisiae* α factor was efficiently coimmunoprecipitated, indicating that a lectin interaction with CLNX may be at play. These results demonstrate that CLNX specifically interacts with SERCA2b and that mutagenesis of N1036 in SERCA2b drastically interferes with this interaction, possibly by changing the charge at the COOH terminus of the Ca^{2+} ATPase.

Phosphorylation in the Cytosolic Domain of CLNX Regulates the Inhibition of Ca^{2+} Oscillations

Stimulation of the IP_3-mediated Ca^{2+} signaling cascade activates PKC, which subsequently phosphorylates downstream targets (Berridge and Irvine, 1989; Berridge, 1993; Newton, 1995). The presence of consensus sites for phosphorylation by PKC/PDK in the cytosolic domain of CLNX raises the possibility that their state of phosphorylation modulates ER lumenal interactions with SERCA2b. To test this hypothesis, we first generated mutants of CLNX in which PKC/PDK consensus phosphorylation sites were changed to unreactive alanines (Fig. 5). We then confocally imaged IP_3-induced Ca^{2+} release in oocytes that were coexpressing these CLNX mutants with SERCA2b, and compared their activity to oocytes coexpressing wild-type CLNX + SERCA2b. Interestingly, the CLNX-S562A mutant did not inhibit Ca^{2+} oscillations (Fig. 6 a). The percentage of oocytes overexpressing CLNX-S562A + SERCA2b that exhibited Ca^{2+} oscillations was indistinguishable from that of control oocytes overexpressing SERCA2b alone, and more importantly, was significantly greater than that of oocytes coexpressing wild-type CLNX + SERCA2b (Fig. 6 b and Table I). These results suggest that phosphorylation of the distal conserved PKC phosphorylation site regulates the inhibition of Ca^{2+} oscillations from the cytosol.

To determine whether the second PKC phosphorylation consensus site is functional, we overexpressed CLNXS 485A + SERCA2b in oocytes. In contrast to what was observed with the CLNX-S562A mutant, repetitive Ca^{2+} waves were inhibited in oocytes overexpressing CLNX-S485A + SERCA2b (n = 27, 85%) (Fig. 6 and Table I). This percentage does not differ significantly from that obtained for oocytes overexpressing CLNX + SERCA2b. This observation is consistent with two hypothetical scenarios. The S485 residue is not functional and the inhibition of Ca^{2+} oscillations can be attributed solely to the distal phosphorylated S562, or S485 is required for the regulation of Ca^{2+} oscillations by S562. To determine which of these two hypotheses was correct, we generated a double mutant in which both serine residues were mutated to alanines (mutant CLNX-S485A/S562A) (Fig. 5). Ca^{2+} wave activity was imaged in oocytes either coexpressing CLNX-S485A/S562A + SERCA2b or overexpressing SERCA2b by itself (Fig. 6 and Table I). Ca^{2+} oscillations were inhibited in the CLNX-S485A/S562A + SERCA2b coexpressing oocytes, suggesting that S485 enables regulation of repetitive Ca^{2+} waves by the S562 residue. Furthermore, the data are consistent with the modulation of Ca^{2+} oscillations by CRT reported previously (Camacho and Lechleiter, 1995a), in that the double CLNX mutant displays constitutive chaperone properties that are not regulated by cytosolic phosphorylation. Taken together, our results reveal the presence of a phosphorylation-dependent regulatory switch in the S562 residue of CLNX.

A Cytosolic Domain Peptide of CLNX Removes the Inhibition of Ca^{2+} Oscillations

A dominant-negative experimental approach was adopted to further implicate an endogenous kinase/phosphatase operating on S562. We hypothesized that coexpression of CLNX with a peptide encompassing the distal PKC/PDK consensus site would compete with the responsible kinase/phosphatase to abrogate the inhibitory effect of CLNX on

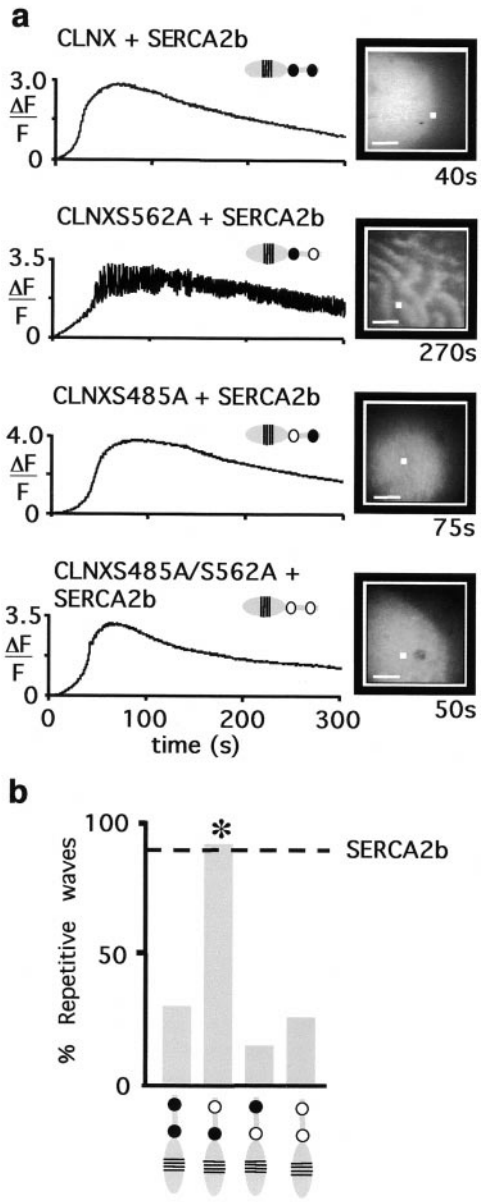

Figure 6. Inhibition of repetitive Ca^{2+} waves is abrogated by a single amino acid mutation in serine residue 562 of CLNX. (a) Changes in fluorescence from resting levels (ΔF/F) are shown for oocytes as labeled. To the right of each trace, a single confocal image of Ca^{2+} wave activity at the indicated time is shown for each representative oocyte. (b) The percentage of oocytes exhibiting repetitive Ca^{2+} wave activity in oocytes coexpressing CLNX-S562A + SERCA2b is increased from that of the wild-type CLNX, and reaches the levels of SERCA2b alone control oocytes (depicted as a dashed line). This percentage was not significantly different in oocytes overexpressing the proximal PKC mutant CLNX-S485A + SERCA2b or the double mutant CLNX-S485A/S562A + SERCA2b when compared with oocytes overexpressing wild-type CLNX + SERCA2b. The asterisk denotes a statistical significant difference ($P < 0.005$, Chi-square) for the comparison of CLNX-S562A mutant to wild-type CLNX.

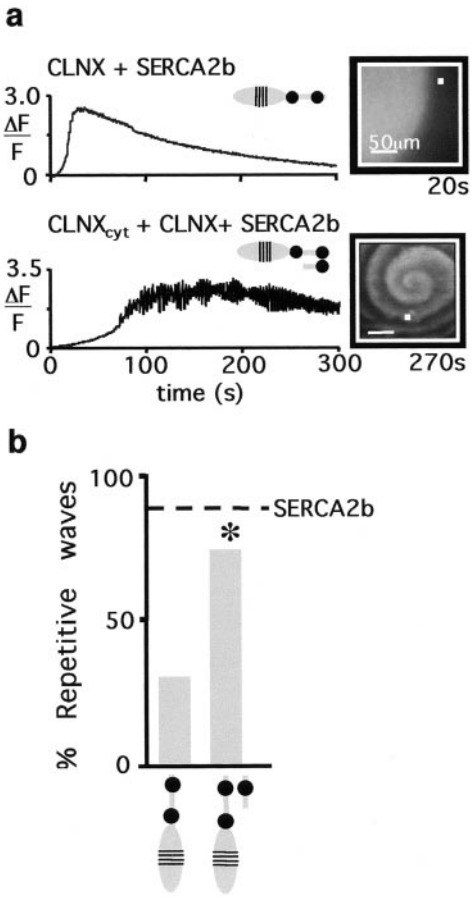

Figure 7. Dominant-negative expression of a competing peptide spanning serine residue 562 of CLNX reverses the inhibition of Ca^{2+} oscillations by the wild-type protein. (a) ΔF/F is shown for a representative control oocyte coexpressing CLNX + SERCA2b (upper panel) and for an oocyte overexpressing $CLNX_{cyt}$ + CLNX + SERCA2b (lower panel). To the right of each trace, a corresponding single confocal image of Ca^{2+} wave activity is shown. (b) The percentage of oocytes exhibiting repetitive Ca^{2+} wave in oocytes coexpressing CLNX + SERCA2b + $CLNX_{cyt}$ is increased when compared with oocytes in which the cytosolic peptide was omitted (CLNX + SERCA2b). The asterisk indicates statistical significance of $P < 0.005$ (Chi-square) for a comparison between oocytes overexpressing $CLNX_{cyt}$ + CLNX + SERCA2b and control oocytes in which the cytosolic peptide was omitted.

Ca^{2+} oscillations. Thus, we engineered a *Xenopus* vector for expression of a cytosolic CLNX peptide, encompassing amino acids 534–571 of mature rat CLNX ($CLNX_{cyt}$). In these experiments, oocytes were injected with mRNA encoding wild-type CLNX + SERCA2b. 18 h before imaging of Ca^{2+} wave activity, mRNA encoding $CLNX_{cyt}$ was injected into half of the experimental oocytes. As predicted, coexpression of the peptide with full-length CLNX + SERCA2b resulted in the abrogation of the inhibitory effects imparted by wild-type CLNX (Fig. 7 a). The percentage of oocytes exhibiting repetitive Ca^{2+} waves increased from 30% in CLNX + SERCA2b coexpressing oocytes to 72% in oocytes that, in addition, coexpressed $CLNX_{cyt}$ ($n = 18$) (Fig. 7 b and Table I). Thus, the cytosolic peptide successfully competes for the endogenous cytosolic kinase/phosphatase that determines the phosphorylation status of S562 and the regulation of Ca^{2+} oscillations.

IP_3-mediated Ca^{2+} Mobilization Causes Dephosphorylation of the Cytosolic Domain of CLNX

Having established the unique contribution of CLNX residue S562 in the inhibition of Ca^{2+} oscillations, we determined the state of phosphorylation of wild-type and CLNX-S562 before and after mobilization of Ca^{2+} by IP_3. This was accomplished by first injecting [γ-^{32}P]ATP into oocytes that were coexpressing CLNX or its S562A mutant, with SERCA2b. Half of the oocytes for each experimental condition was subsequently injected with IP_3 ($\sim$300 nM final). Immunoprecipitations with a CLNX-specific antibody were then carried out. Similar measurements were also performed in oocytes coexpressing the cytosolic peptide $CLNX_{cyt}$ with wild-type CLNX (Fig. 8 a). In control oocytes overexpressing SERCA2b alone, CLNX was not detected. Interestingly, CLNX was phosphorylated under resting conditions and was dephosphorylated by IP_3-mediated mobilization of Ca^{2+}. Basal phosphorylation of the S562A mutant was less than half of wild-type CLNX and was not changed by IP_3 injection. These observations suggest first that the S562 residue is phosphorylated, and second that the Ca^{2+}-sensitive dephosphorylation of CLNX is specific for this residue. Under resting conditions, phosphorylation of CLNX was slightly reduced by coexpression with the $CLNX_{cyt}$ peptide, and after IP_3 injection, there was a further reduction in the level of phosphorylation seen. This suggests that the function of the $CLNX_{cyt}$ peptide was to compete with the phosphatase activity responsible for CLNX dephosphorylation. Data from oocytes expressing the S485A and S485A/S562A mutants of CLNX are not shown, since the level of phosphate label detected was too low to reliably demonstrate the phosphorylation status of either mutant, consistent with the report by Wong et al. (1998).

Western blot analysis with an anti-CLNX antibody was performed on oocyte fractions coexpressing CLNX or its PKC/PDK phosphorylation mutants, with SERCA2b (Fig. 8 b). A single band migrating at $\sim$90 kD was observed in membrane extracts prepared from oocytes overexpressing CLNX or its mutants, consistent with the reported molecular weight for CLNX (Wada et al., 1991). Thus, the differences in intensity of phosphorylated CLNX and its mutants cannot be attributed to differences in overexpression levels. In control oocyte extracts overexpressing SERCA2b alone, no detectable CLNX immunoreactivity was observed. To determine whether SERCA2b was coexpressed with CLNX, we probed oocyte extracts with an anti–rat SERCA2b antibody (John et al., 1998). SERCA2b overexpression was demonstrated in all extracts (Fig. 8 c). We observed no significant differences in SERCA2b immunoreactivity. When small variations did occur, they did not correlate with the presence or absence of Ca^{2+} oscillations. In particular, notice that the SERCA2b immunoreactivity detected in extracts from CLNX-S562A + SERCA2b overexpressing oocytes was slightly lower, but these levels of SERCA2b expression did not correlate with a decrease in the frequency of Ca^{2+} oscillations.

The Interaction of CLNX with SERCA2b Is Reduced by Dephosphorylation Treatment

To determine whether cytosolic dephosphorylation of

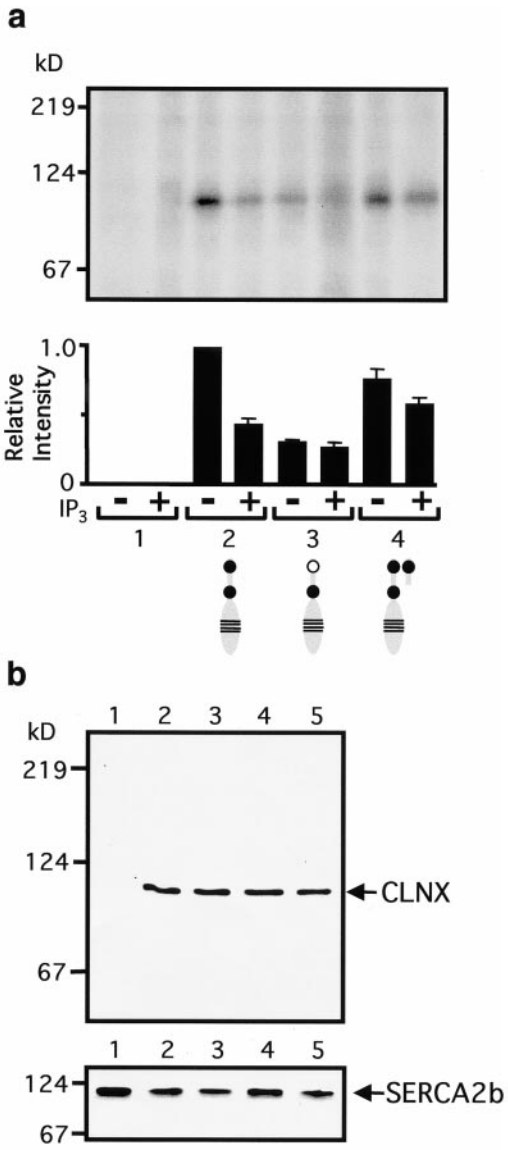

Figure 8. CLNX is dephosphorylated after IP_3 injection. (a) Immunoprecipitations of [γ-^{32}P]ATP-labeled CLNX and CLNX-S562A mutant from oocytes injected with IP_3 (+) or noninjected (−) control oocytes run on SDS-PAGE (upper panel). Paired samples were loaded ± IP_3 for oocytes overexpressing the following: SERCA2b alone (first set of lanes), CLNX + SERCA2b (second set of lanes), CLNX-S562A + SERCA2b (third set of lanes), and $CLNX_{cyt}$ + CLNX + SERCA2b (fourth set of lanes). Densitometric analysis of the phosphorylated protein bands was normalized to the intensity of the wild-type CLNX ($-IP_3$) and plotted in arbitrary units (lower panel). (b) Immunodetection of CLNX detected by Western blotting in oocytes overexpressing the following: CLNX and CLNX mutants with SERCA2b (upper panel). The gel was loaded as follows: SERCA2b (lane 1), CLNX + SERCA2b (lane 2), CLNX-S485A/S562A + SERCA2b (lane 3), CLNX-S485A + SERCA2b (lane 4), and CLNX-S562A + SERCA2b (lane 5). Immunodetection of SERCA2b in oocytes coexpressing SERCA2b with CLNX and CLNX mutants (lower panel). The lanes correspond to protein fractions from oocytes that were injected with mRNAs encoding the following: SERCA2b (lane 1), CLNX + SERCA2b (lane 2), CLNX-S562A + SERCA2b (lane 3), CLNX-S485A + SERCA2b (lane 4), and CLNX-S485A/S562A + SERCA2b (lane 5).

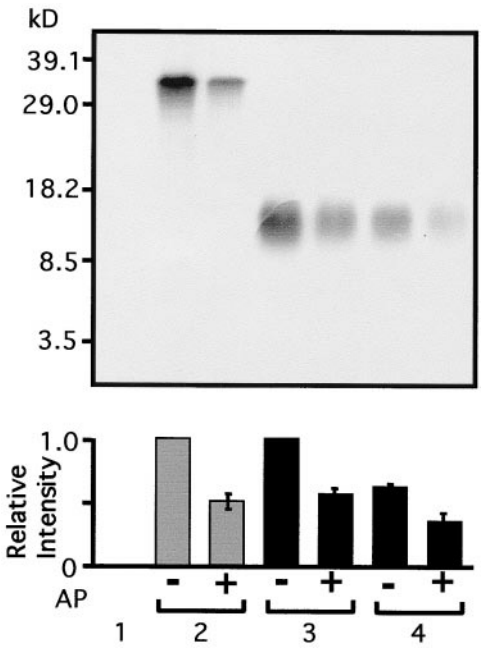

Figure 9. Dephosphorylation of CLNX reduces its interaction with SERCA2b. In vitro translations of synthetic mRNAs were performed in rabbit reticulocyte lysate supplemented with canine pancreatic microsomes and L-[^{35}S]methionine. Isolated microsomes were treated with alkaline phosphatase as described in Materials and Methods, the samples were subjected to 15% SDS-PAGE, and detected by fluorography. A positive glycosylation control of *S. cerevisiae* α factor was also translated. Paired samples ± alkaline phosphatase treatment that were coimmunoprecipitated with CLNX were loaded in the following order: negative control without RNA in the translation (lane 1), *S. cerevisiae* α factor (second set of lanes), SERCA2b/TM9-11 (third set of lanes), and SERCA2b-N1036A/TM9-11 (fourth set of lanes).

CLNX affects its interaction with SERCA2b, we immunoprecipitated endogenous CLNX from microsomes treated with alkaline phosphatase and detected proteins bound to CLNX by fluorography (Fig. 9). Calf intestinal phosphatase removes phosphate groups from phosphoserine and phosphothreonine residues, which accounts for >97% of phosphate bound to eukaryotic cells. The microsomes were isolated from translation reactions programmed to express the COOH terminus of SERCA2b (TM9-11) and *S. cerevisiae* α factor as a positive control. Interestingly, alkaline phosphatase treatment significantly reduced the coimmunoprecipitation of both substrates with CLNX, suggesting that in the dephosphorylated state CLNX no longer associates with the SERCA2b substrate.

Discussion

In this study, we demonstrated that CLNX overexpression in *Xenopus* oocytes modulates IP_3-mediated Ca^{2+} oscillations. As observed for CRT, modulation of Ca^{2+} release is manifested by an inhibition of repetitive Ca^{2+} waves in a manner consistent with inhibition of SERCA2b activity (Camacho and Lechleiter, 1995a; John et al., 1998). More importantly, unlike the modulation by CRT, the inhibition of Ca^{2+} oscillations by CLNX is subject to regulation by the phosphorylation status of its cytosolic domain.

Store refilling by SERCA pumps is the predominant factor that controls the frequency of Ca^{2+} oscillations (Camacho and Lechleiter, 1993). Consistent with this, we find that overexpression of SERCA2b alone results in ~90% of oocytes exhibiting high-frequency Ca^{2+} waves, whereas coexpression of CLNX + SERCA2b reduces this number to 30%. Detailed analysis of Ca^{2+} wave activity in CLNX + SERCA2b overexpressing oocytes that did not show complete inhibition also revealed an effect consistent with inhibition of the Ca^{2+} ATPase. Specifically, we found statistically significant increases in wave periods and the $t_{1/2}$ decay of individual waves when CLNX was coexpressed with SERCA2b. Both of these parameters are indicators of the refilling process. Furthermore, the inhibition of Ca^{2+} oscillations was equally manifested regardless of whether the oscillations were generated by overexpression of SERCA2b pumps or whether mitochondria were energized.

We have shown previously that CRT inhibition of Ca^{2+} oscillations is dependent on the presence of a lumenal asparagine in SERCA2b (N1036), which appeared to be targeted by the chaperone (John et al., 1998). Here we found that in oocytes coexpressing CLNX + SERCA2b-N1036, Ca^{2+} oscillations were not inhibited, suggesting that both members of this family of proteins inhibit Ca^{2+} oscillations by similar mechanisms. We found that there is a physical interaction of CLNX with the COOH terminus of SERCA2b which is reduced by mutagenesis on N1036A and is not at all existent with SERCA2a. This reduction in the interaction may be due to a change in charge induced by mutagenesis of SERCA2b-N1036A, since we found no evidence that SERCA2b was glycosylated on N1036. Together, these results raise the possibility that CLNX inhibition of Ca^{2+} oscillations is due to a protein–protein interaction with the COOH terminus of SERCA2b. Recently, Ihara et al. reported that CLNX is a classical molecular chaperone in that it can operate independently of the state of glycosylation of target proteins (Ihara et al., 1999). The authors suggest that CLNX recognizes exposed hydrophobic pockets in substrate proteins maintaining them in a folding-competent state. It is then possible that proteins residing in the ER might benefit from the chaperone activity of CLNX to allow them to function in the oxidizing/gel matrix of the ER.

CLNX was first characterized as a phosphoprotein in the ER (Wada et al., 1991) and more recently, efforts have been directed to identify the specific residues that support phosphorylation (Wong et al., 1998). In particular, these authors described three phosphorylatable residues in the cytosolic domain of dog CLNX, including the homologous residue to S562 in rat CLNX. They demonstrate that phosphorylation of S562 modulates the interaction of CLNX with the ribosome. Here, we discovered by site-directed mutagenesis that the S562 in CLNX supports phosphorylation with functional consequences for the control of Ca^{2+} oscillations. Specifically, unlike the inhibition of repetitive Ca^{2+} waves observed in oocytes overexpressing CLNX + SERCA2b, the frequency of repetitive waves observed in oocytes overexpressing CLNX-S562A + SERCA2b is similar to that of the Ca^{2+} ATPase expressed

alone. In addition, dominant-negative expression of a peptide encompassing this PKC/PDK phosphorylation site of CLNX relieved the inhibition of Ca^{2+} oscillations imparted by the wild-type chaperone. From these results, we conclude that S562 in the cytosolic domain of CLNX is a molecular switch that controls Ca^{2+} oscillations. Our results suggest that dephosphorylation of S562 removes the functional interaction of the chaperone with SERCA2b, resulting in a pump that is no longer inhibited. CLNX has a second consensus site for phosphorylation by PKC (S485), although it is not known whether it is functional. Coexpression of the S485A mutant with SERCA2b decreased the number of oocytes that displayed repetitive waves to 15%, suggesting stronger inhibition of the pump. Two interpretations are possible for this finding. Either S485 has opposite effects to S562, or it is nonfunctional. We resolved this issue by coexpressing the double mutant CLNX-S562A/S485A with SERCA2b, which also resulted in inhibition of Ca^{2+} oscillations. This result suggests that the S485 residue is required for the regulation of the Ca^{2+} oscillations upon dephosphorylation of the distal S562 residue. Interestingly, this proposed mechanism of action is reminiscent of the relief from inhibition of SERCA2a after store depletion in cardiac muscle (Bhogal and Colyer, 1998). In this tissue, phosphorylation of phospholamban is responsible for relief of inhibition of the pump, although a chaperone interaction is not involved (Jackson and Colyer, 1996; MacLennan and Toyofuku, 1996). Thus, CLNX appears to be the functional equivalent of phospholamban in nonmuscle cells, where it provides phosphorylation-

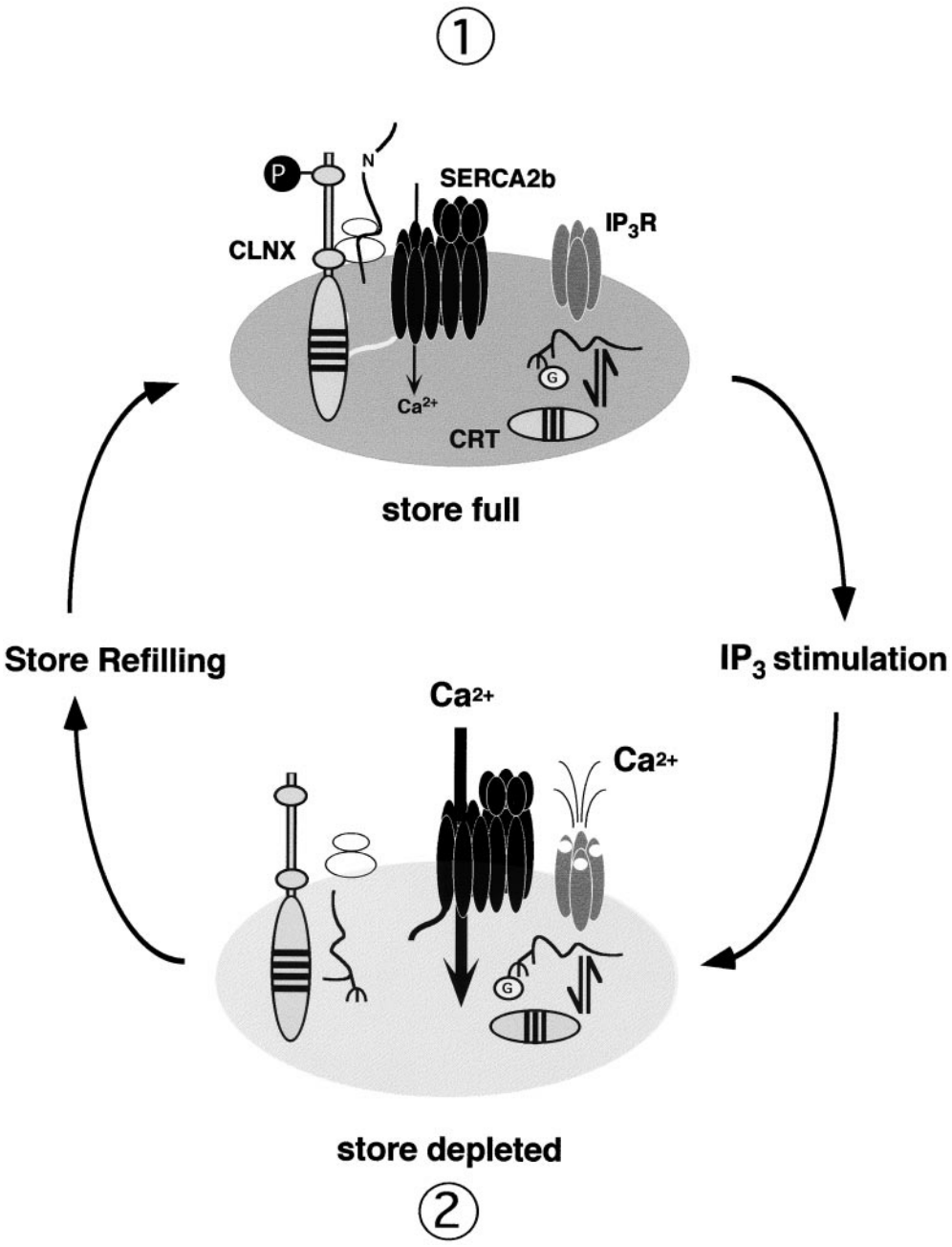

Figure 10. Model depicting the functional consequences of cytosolic phosphorylation of CLNX. (1) Under resting conditions, CLNX is phosphorylated on S562 located in the cytosolic domain of CLNX as shown. In this state, we suggest that CLNX is free to interact with the COOH terminus of SERCA2b. CLNX may also interact with the ribosome. The Ca^{2+} ATPase is inhibited, the Ca^{2+} stores are expected to be full (dark gray) and in an optimal condition for protein folding. (2) Mobilization of the Ca^{2+} stores by IP_3 (light gray) results in a Ca^{2+}-dependent dephosphorylation of S562 in CLNX. In the dephosphorylated state, inhibition of repetitive Ca^{2+} waves by CLNX is not observed, suggesting a loss of interaction with the pump resulting in Ca^{2+} store refilling. This phosphorylation switch implies that cytosolic Ca^{2+} regulates interactions of CLNX with lumenal proteins (e.g., SERCA2b), resulting in control of Ca^{2+} uptake and also modulation of protein folding in the ER lumen. In contrast, a bi-directional arrow is shown to indicate that the interaction of CRT with targets is determined by lumenal conditions. (See Discussion for further details).

dependent regulation of Ca^{2+} uptake by SERCA2b. Furthermore, the mutants S485A and S485A/S562A behaved like CRT, which lacks cytosolic regulation and is consistent with the observation that a soluble ER lumenal domain of CLNX (ΔTMC), which promotes refolding of ribonuclease B, acts like CRT (Zapun et al., 1997).

The serine residues characterized here conform to a consensus motif for PKC/PDK phosphorylation (Wong et al., 1998). From a signaling perspective, activation of the IP_3 pathway would be expected, via PKC, to provide Ca^{2+}-mediated feedback to regulate downstream phosphorylatable targets such as CLNX. To test this hypothesis, immunoprecipitations of CLNX and CLNX-S562A mutant were performed from membrane fractions of [^{32}P]ATP-labeled oocytes in the presence or absence of IP_3. These studies revealed that wild-type CLNX was phosphorylated under resting conditions and dephosphorylated after IP_3 injection. Furthermore, the detected phosphate label is on S562, since CLNX-S562A has a corresponding decrease in the amount of phosphate at rest, and more significantly, there is no further decrease upon stimulation by IP_3. We find that treatment with calf intestinal alkaline phosphatase decreases the interaction of CLNX with the COOH terminus of SERCA2b. This is consistent with the possibility that dephosphorylation of S562 is transduced to the ER lumen, causing dissociation of CLNX from SERCA2b. The phosphatase responsible for the Ca^{2+}-dependent dephosphorylation of CLNX remains to be identified. A candidate for this role may be the Ca^{2+}-dependent phosphatase, calcineurin (Klee et al., 1998). Recently, Chevet et al. demonstrated that the equivalent residue in dog CLNX is phosphorylated by extracellular-signal regulated kinase 1 (ERK-1), and interestingly, phosphorylation by ERK-1 and CKII increased CLNX association with ribosomes in pancreatic microsomes (Chevet et al., 1999). The kinase responsible for phosphorylation of S562 remains to be identified in the oocyte.

One of the major implications of our study is that CRT should be viewed as a chaperone that is strictly controlled by ER lumenal conditions such as Ca^{2+} and interactions with other proteins (Corbett et al., 1999). In contrast, CLNX, via phosphorylation of its cytosolic domain, introduces an additional level of complexity to the signaling that controls protein processing. In Fig. 10, we present a model describing the Ca^{2+}-dependent regulation via cytosolic phosphorylation of the interaction of CLNX with SERCA2b. In this model, we also attempt to incorporate the recent findings of Chevet et al. (1999) regarding the phosphorylation-dependent interaction of CLNX with the ribosome. We suggest that in the resting state (1), CLNX is phosphorylated on S562 and the Ca^{2+} stores are full. Furthermore, CLNX is interacting with SERCA2b at the COOH lumenal terminus, keeping the pump in an inhibited state. CLNX may also be bound to the ribosome maintaining optimal conditions for folding of newly synthesized proteins as they translocate into the ER. Upon mobilization of Ca^{2+} from internal stores by IP_3 (2), cytosolic Ca^{2+} is increased, activating a phosphatase that dephosphorylates CLNX, removing its interaction with SERCA2b, and allowing the pump to refill the Ca^{2+} stores. Dephosphorylation of CLNX also causes its dissociation from the ribosome (Chevet et al., 1999). Since protein translation is inhibited after store depletion, an interaction between CLNX and the ribosome is no longer required (Reilly et al., 1998). Restoration of ER lumenal Ca^{2+} has interesting consequences for the maintenance of ER protein folding. Lumenal Ca^{2+} is required for association of the lectin chaperones with misfolded targets, and more importantly, it is required for the action of the UDP-Glc glycoprotein glucosyl transferase (Trombetta and Parodi, 1992). Furthermore, depletion of Ca^{2+} from internal stores causes accumulation of misfolded proteins in the ER (Lodish and Kong, 1990; Lodish et al., 1992; Choudhury et al., 1997) and upregulation of CRT expression at the mRNA and protein levels within a few hours (Llewellyn et al., 1996; Waser et al., 1997). Likewise, CLNX isoforms in yeast are induced by ER stress (Jannatipour and Rokeach, 1995). Our data are consistent with the idea that dephosphorylation of CLNX is an acute response (minutes) to Ca^{2+} store depletion, and removal of pump inhibition then ensures optimal ER lumenal conditions for protein folding. We suggest that folding events in the ER lumen are under the control of the IP_3-mediated Ca^{2+} signaling system. Since these chaperones in turn modulate cytosolic Ca^{2+} by virtue of their putative luminal interactions with the SERCA2b, this system represents a novel bi-directional mode of signaling between the ER and the cytosol.

We wish to thank E. Nasi and D. Castle for critical reading of the manuscript. We are grateful to the following individuals for kindly providing reagents: L. Tjoelker (rat calnexin cDNA), J. Bergeron (anti-calnexin antibody), and J. Lytton (anti-SERCA2 antibody). We also thank Clarise Rivera and Margaret Zembala for their technical support.

This work was funded the National Institutes of Health grant R01 GM55372 to P. Camacho.

Submitted: 26 April 2000
Accepted: 2 May 2000

References

Baksh, S., and M. Michalak. 1991. Expression of calreticulin in *Escherichia coli* and identification of its Ca^{2+} binding domains. *J. Biol. Chem.* 266:21458–21465.

Bastianutto, C., E. Clementi, F. Codazzi, P. Podini, F. De Giorgi, R. Rizzuto, J. Meldolesi, and T. Pozzan, 1995. Overexpression of calreticulin increases the Ca^{2+} capacity of rapidly exchanging Ca^{2+} stores and reveals aspects of their luminal microenvironment and function. *J. Cell Biol.* 130:847–855.

Bayle, D., D. Weeks, and G. Sachs. 1995. The membrane topology of the rat sarcoplasmic and endoplasmic reticulum calcium ATPases by in vitro translation scanning. *J. Biol. Chem.* 270:25678–25684.

Bergeron, J.J.M., M.B. Brenner, D.Y. Thomas, and D.B. Williams. 1994. Calnexin: a membrane-bound chaperone of the endoplasmic reticulum. *Trends Biochem. Sci.* 19:124–128.

Berridge, M.J. 1993. Inositol trisphosphate and calcium signalling. *Nature.* 361: 315–325.

Berridge, M.J., and R.F. Irvine. 1989. Inositol phosphates and cell signaling. *Nature.* 341:197–205.

Bezprozvanny, I., J. Watras, and B.E. Ehrlich. 1991. Bell-shaped calcium-response curves of Ins(1,4,5)P_3- and calcium-gated channels from endoplasmic reticulum of cerebellum. *Nature.* 351:751–754.

Bhogal, M.S., and J. Colyer. 1998. Depletion of Ca^{2+} from the sarcoplasmic reticulum of cardiac muscle prompts phosphorylation of phospholamban to stimulate store refilling. *Proc. Natl. Acad. Sci. USA.* 95:1484–1489.

Camacho, P., and J. Lechleiter. 1993. Increased frequency of calcium waves in *Xenopus laevis* oocytes that express a calcium-ATPase. *Science.* 260:226–229.

Camacho, P., and J.D. Lechleiter. 1995a. Calreticulin inhibits repetitive calcium waves. *Cell.* 82:765–771.

Camacho, P., and J.D. Lechleiter. 1995b. Spiral calcium waves: implications for signalling. *In* Calcium Waves, Gradients and Oscillations - Symposium No. 188. G. Bock and K. Ackrill, editors. John Wiley & Son, Ltd., New York. 66–84.

Chevet, E., H.N. Wong, D. Gerber, C. Cochet, A. Fazel, P.H. Cameron, J.N.

Gushue, D.Y. Thomas, and J.J. Bergeron. 1999. Phosphorylation by CK2 and MAPK enhances calnexin association with ribosomes. *EMBO (Eur. Mol. Biol. Organ.) J.* 18:3655–3666.

Choudhury, P., Y. Liu, R.J. Bick, and R.N. Sifers. 1997. Intracellular association between UDP-glucose:glycoprotein glucosyltransferase and an incompletely folded variant of alpha1-antitrypsin. *J. Biol. Chem.* 272:13446–13451.

Coppolino, M.G., M.J. Woodside, N. Demaurex, S. Grinstein, R. St-Arnaud, and S. Dedhar. 1997. Calreticulin is essential for integrin-mediated calcium signalling and cell adhesion. *Nature.* 386:843–847.

Corbett, E.F., K. Oikawa, P. Francois, D.C. Tessier, C. Kay, J.J. Bergeron, D.Y. Thomas, K.H. Krause, and M. Michalak. 1999. Ca^{2+} regulation of interactions between endoplasmic reticulum chaperones. *J. Biol. Chem.* 274:6203–6211.

Dolmetsch, R.E., K. Xu, and R.S. Lewis. 1998. Calcium oscillations increase the efficiency and specificity of gene expression. *Nature.* 392:933–936.

Fasolato, C., P. Pizzo, and T. Pozzan. 1998. Delayed activation of the store-operated calcium current induced by calreticulin overexpression in RBL-1 cells. *Mol. Biol. Cell.* 9:1513–1522.

Finch, E.A., T.J. Turner, and S.M. Goldin. 1991. Calcium as a coagonist of inositol 1,4,5-trisphosphate-induced calcium release. *Science.* 252:443–446.

Fliegel, L., K. Burns, D.H. MacLennan, R.A.F. Reithmeier, and M. Michalak. 1989. Molecular cloning of the high affinity calcium binding protein (calreticulin) of skeletal muscle sarcoplasmic reticulum. *J. Biol. Chem.* 264:21522–21528.

Gomez, T.M., and N.C. Spitzer. 1999. In vivo regulation of axon extension and pathfinding by growth-cone calcium transients. *Nature.* 397:350–355.

Gunteski-Hamblin, A.-M., J. Greeb, and G.E. Shull. 1988. A novel Ca^{2+} pump expressed in brain, kidney, and stomach is encoded by an alternative transcript of the slow-twitch muscle sarcoplasmic reticulum Ca-ATPase gene. *J. Biol. Chem.* 263:15032–15040.

Helenius, A., E.S. Trombetta, D.N. Hebert, and J.F. Simmons. 1997. Calnexin, calreticulin, and the folding of glycoproteins. *Trends Cell Biol.* 7:193–200.

Ihara, Y., M.F. Cohen-Doyle, Y. Saito, and D.B. Williams. 1999. Calnexin discriminates between protein conformational states and functions as a molecular chaperone in vitro. *Mol. Cell.* 4:331–341.

Iino, M. 1990. Biphasic Ca^{2+} dependence of inositol 1,4,5-trisphosphate-induced Ca^{2+} release in smooth muscle cells of the guinea pig *taenia caeci. J. Gen. Physiol.* 95:1103–1122.

Jackson, W.A., and J. Colyer. 1996. Translation of Ser16 and Thr17 phosphorylation of phospholamban into Ca^{2+}-pump stimulation. *Biochem. J.* 316:201–207.

Jannatipour, M., and L.A. Rokeach. 1995. The *Schizosaccharomyces pombe* homologue of the chaperone calnexin is essential for viability. *J. Biol. Chem.* 270:4845–4853.

John, L.M., J.D. Lechleiter, and P. Camacho. 1998. Differential modulation of SERCA2 isoforms by calreticulin. *J. Cell Biol.* 142:963–973.

Jouaville, L.S., F. Ichas, E.L. Holmuhamedov, P. Camacho, and J.D. Lechleiter. 1995. Synchronization of calcium waves by mitochondrial substrates in *Xenopus laevis. Nature.* 377:438–441.

Klee, C.B., H. Ren, and X. Wang. 1998. Regulation of the calmodulin-stimulated protein phosphatase, calcineurin. *J. Biol. Chem.* 273:13367–13370.

Li, W., J. Llopis, M. Whitney, G. Zlokarnik, and R.Y. Tsien. 1998. Cell-permeant caged InsP3 ester shows that Ca^{2+} spike frequency can optimize gene expression. *Nature.* 392:936–941.

Llewellyn, D.H., J.M. Kendall, F.N. Sheikh, and A.K. Campbell. 1996. Induction of calreticulin expression in HeLa cells by depletion of the endoplasmic reticulum Ca^{2+} store and inhibition of N-linked glycosylation. *Biochem. J.* 318:555–560.

Lodish, H.F., and N. Kong. 1990. Perturbation of cellular calcium blocks exit of secretory proteins from the rough endoplasmic reticulum. *J. Biol. Chem.* 265:10893–10899.

Lodish, H.F., N. Kong, and L. Wikstrom. 1992. Calcium is required for folding of newly made subunits of the asialoglycoprotein receptor within the endoplasmic reticulum. *J. Biol. Chem.* 267:12753–12760.

MacLennan, D.H., and T. Toyofuku. 1996. Regulatory interactions between calcium ATPases and phospholamban. *Soc. Gen. Physio. Ser.* 51:89–103.

MacLennan, D.H., W.J. Rice, and N.M. Green. 1997. The mechanism of Ca^{2+} transport by sarco(endo)plasmic reticulum Ca^{2+}-ATPases. *J. Biol. Chem.* 272:28815–28818.

Mery, L., N. Mesaeli, M. Michalak, M. Opas, D. Lew, and K.-H. Krause. 1996. Overexpression of calreticulin increases intracellular Ca^{2+} storage and decreases store-operated Ca^{2+} influx. *J. Biol. Chem.* 271:9322–9339.

Mesaeli, N., K. Nakamura, E. Zvaritch, P. Dickie, E. Dziak, K.H. Krause, M. Opas, D.H. MacLennan, and M. Michalak. 1999. Calreticulin is essential for cardiac development. *J. Cell Biol.* 144:857–868.

Michalak, M., R.E. Milner, K. Burns, and M. Opas. 1992. Calreticulin. *Biochem. J.* 285:681–692.

Newton, A.C. 1995. Protein kinase C: structure, function and regulation. *J. Biol. Chem.* 270:28495–28498.

Ohsako, S., Y. Hayashi, and D. Bunick. 1994. Molecular cloning and sequencing of calnexin-t. An abundant male germ cell-specific calcium-binding protein of the endoplasmic reticulum. *J. Biol. Chem.* 269:14140–14148.

Oliver, J.D., R.C. Hresko, M. Mueckler, and S. High. 1996. The glut 1 glucose transporter interacts with calnexin and calreticulin. *J. Biol. Chem.* 271: 13691–13696.

Parker, I., and I. Ivorra. 1990. Inhibition by Ca^{2+} of inositol trisphosphate-mediated Ca^{2+} liberation: a possible mechanism for oscillatory release of Ca^{2+}. *Proc. Natl. Acad. Sci. USA.* 87:260–264.

Reilly, B.A., M.A. Brostrom, and C.O. Brostrom. 1998. Regulation of protein synthesis in ventricular myocytes by vasopressin. The role of sarcoplasmic/endoplasmic reticulum Ca^{2+} stores. *J. Biol. Chem.* 273:3747–3755.

Robb-Gaspers, L.D., P. Burnett, G.A. Rutter, R.M. Denton, R. Rizzuto, and A.P. Thomas. 1998. Integrating cytosolic calcium signals into mitochondrial metabolic responses. *EMBO (Eur. Mol. Biol. Organ.) J.* 17:4987–5000.

Roderick, H.L., D.H. Llewellyn, A.K. Campbell, and J.M. Kendall. 1998. Role of calreticulin in regulating intracellular Ca^{2+} storage and capacitative Ca^{2+} entry in HeLa cells. *Cell Calcium.* 24:253–262.

Tjoelker, L.W., C.E. Seyfried, R.L. Eddy, Jr., M.G. Byers, T.B. Shows, J. Calderon, R.B. Schreiber, and P.W. Gray. 1994. Human, mouse, and rat calnexin cDNA cloning: identification of potential calcium binding motifs and gene localization to human chromosome 5. *Biochemistry.* 33:3229–3236.

Trombetta, S.E., and A.J. Parodi. 1992. Purification to apparent homogeneity and partial characterization of rat liver UDP-glucose:glycoprotein glucosyltransferase. *J. Biol. Chem.* 267:9236–9240.

Vassilakos, A., M. Michalak, M.A. Lehrman, and D.B. Williams. 1998. Oligosaccharide binding characteristics of the molecular chaperones calnexin and calreticulin. *Biochemistry.* 37:3480–3490.

Wada, I., D. Rindress, P.H. Cameron, W.J. Ou, J.J. Doherty II, D. Louvard, A.W. Bell, D. Dignard, D.Y. Thomas, and J.J. Bergeron. 1991. SSR alpha and associated calnexin are major calcium binding proteins of the endoplasmic reticulum membrane. *J. Biol. Chem.* 266:19599–19610.

Waser, M., N. Mesaeli, C. Spencer, and M. Michalak. 1997. Regulation of calreticulin gene expression by calcium. *J. Cell Biol.* 138:547–557.

Watanabe, D., K. Yamada, Y. Nishina, Y. Tajima, U. Koshimizu, A. Nagata, and Y. Nishimune. 1994. Molecular cloning of a novel Ca^{2+} binding protein (calmegin) specifically expressed during male meiotic germ cell development. *J. Biol. Chem.* 269:7744–7749.

Wong, H.N., M.A. Ward, A.W. Bell, E. Chevet, S. Bains, W.P. Blackstock, R. Solari, D.Y. Thomas, and J.J. Bergeron. 1998. Conserved in vivo phosphorylation of calnexin at casein kinase II sites as well as a protein kinase C/proline-directed kinase site. *J. Biol. Chem.* 273:17227–17235.

Zapun, A., S.M. Petrescu, P.M. Rudd, R.A. Dwek, D.Y. Thomas, and J.J. Bergeron. 1997. Conformation-independent binding of monoglucosylated ribonuclease B to calnexin. *Cell.* 88:29–38.